Sequence specificity for uridylylation of the viral peptide linked to the genome (VPg) of enteroviruses

Catherine H. Schein [a],[*], Mengyi Ye [b], Aniko V. Paul [c], M. Steven Oberste [d], Nora Chapman [e], Gerbrand J. van der Heden van Noort [f], Dmitri V. Filippov [f], Kyung H. Choi [b]

[a] Foundation for Applied Molecular Evolution (FfAME), 13709 Progress Blvd., Alachua, FL 32616, United States
[b] Dept. Biochemistry and Molecular Biology, University of Texas Medical Branch, Galveston, TX 77555, United States
[c] Dept. Molecular Genetics and Microbiology, Stony Brook University, Stony Brook, NY 11790, United States
[d] Division of Viral Diseases, Centers for Disease Control and Prevention, 1600 Clifton Rd NE, MS G-17, Atlanta, GA 30333, United States
[e] Dept. Pathology and Microbiology, University of Nebraska Medical Center, NE 68198, United States
[f] Leiden Institute of Chemistry, Leiden University, P.O. Box 9502, 2300 RA, Leiden, The Netherlands

ARTICLE INFO

ABSTRACT

Enteroviruses (EV) uridylylate a peptide, VPg, as the first step in their replication. VPgpUpU, found free in infected cells, serves as the primer for RNA elongation. The abilities of four polymerases (3D^{pol}), from EV-species A–C, to uridylylate VPgs that varied by up to 60% of their residues were compared. Each 3D^{pol} was able to uridylylate all five VPgs using polyA RNA as template, while showing specificity for its own genome encoded peptide. All 3D^{pol} uridylylated a consensus VPg representing the physical chemical properties of 31 different VPgs. Thus the residues required for uridylylation and the enzymatic mechanism must be similar in diverse EV. As VPg-binding sites differ in co-crystal structures, the reaction is probably done by a second 3D^{pol} molecule. The conservation of polymerase residues whose mutation reduces uridylylation but not RNA elongation is compared.

© 2015 Elsevier Inc. All rights reserved.

Introduction

The human enteroviruses (EV), which include the polioviruses (PV), coxsackie viruses (CVA, CVB) and many other pathogens, cause febrile rash, respiratory illness, and neurologic disease (Eyckmans et al., 2014; Pallansch et al., 2013). Although incidence of PV paralysis has been reduced by >99% globally through routine immunization and mass vaccination campaigns, there continue to be cases in areas where vaccine campaigns have been inhibited by social unrest (Moturi et al., 2014). Non-polio EV, such as EV A71 (Chan et al., 2011; Wang et al., 2014; Yu et al., 2014; Zheng et al., 2014) and EV 68(Stephenson, 2014) (Jacobson et al., 2012; Tokarz et al., 2012) can spread rapidly among children. These can cause severe respiratory illness and a range of neuro-logical diseases, from aseptic meningitis to encephalitis and paralysis (Kreuter et al., 2011; Pallansch et al., 2013; Tao et al., 2014). Infections with other EV, such as CVB3, may contribute to diabetes (Salvatoni et al., 2013; Yeung et al., 2011) and heart disease(Chapman and Kim, 2008; Cooper, 2009).

There are currently no drugs approved for the treatment of the many different enterovirus infections (Abzug, 2014). As EV are omnipresent in the intestinal tract of humans and animals, there is little way to prevent occasional infections. Their antigenic diversity (Acevedo et al., 2014; Blomqvist et al., 2008) makes it difficult to develop vaccines to protect against the many different enterovirus pathogens. To aid in developing more widespread treatments for EV infections (Campagnola et al., 2011), it is important to identify common properties of the viral proteins involved in replication.

Early studies of poliovirus replication revealed that the 5′ end of the RNA was covalently bound to a small peptide, called VPg (for viral protein linked to the genome), which was essential for PV

Virus	VPg Sequence	GenBank Accession #
EV_A71	GAYSGAPKQVLKKPALRTATVQ	AJD77327
EV103	GAYTGLPFNKPKVPTIRQAKVQ	FJ007373
SV6	GAYTGLPFNKPKVPTIRQAKVQ	AF326766
EV108	GAYTGLPFTKPKVPTIRQAKVQ	AF414372
BaEV	GAYSGMPQTKPKVPTIRQAKVQ	AF326750
EV4	GAYTGMPNQKPKVPTLRQAKVQ	AY302557
CVB1	GAYTGMPNQKPKVPTLRQAKVQ	M16560
CVB3	GAYTGVPNQKPRVPTLRQAKVQ	M88483
EV5	GAYTGMPNQKPKVPTLRQAKVQ	AF083069
CVB6	GAYTGMPNQKPKVPTLRQAKVQ	AF039205
EV11	GAYTGMPNQKPKVPTLRQAKVQ	X80059
EV6	GAYTGMPNQKPKVPTLRQARVQ	AY302558
EV3	GAYTGMPNQKPKVPTLRQAKVQ	AY302553
EV7	GAYTGIPNQKPKVPTLRQAKVQ	AY302559
EV87	GAYTGLPNQKPKVPTLRQAKVQ	AY843305
CVB1	GAYTGLPNQKPKVPTLRQAKVQ	AAO84300
EV75	GAYTGMPNQKPKVPTLRQAKVQ	AY556070
EV30	GAYSGMPNQKSKVPTLRQAKVQ	AF162711
CVA20	GAYTGMPNQKPKVPTLRQAKVQ	AF499642
CVA18	GPYTGLPSKKPNIPTIRTAKVQ	BAE20393
CVA17	GAYTGLPNKKPNIPTIRTAKVQ	AF499639
EV102	GAYTGLPNKKPNVPTIRTAKVQ	EF555645
CVA13	GAYTGLPNKRPNVPTIRTAKVQ	AF499637
CVA21	GAYTGLPNKKPNVPTIRVAKVQ	AF546702
CVA11	GAYTGLPNKRPSVPTIRTAKVQ	AF499636
PV3	GAYTGLPNKRPNVPTIRTAKVQ	K01392
PV1	GAYTGLPNKKPNVPTIRTAKVQ	J02281/ V01149
PV2	GAYTGLPNKRPNVPTIRTAKVQ	M12197
CVA15	GAYTGLPNKRPNVPTIRTAKVQ	AF499638
CVA24	GAYTGLPNKKPSVPTVRTAKVQ	D90457
EV96	GAYTGLPSKKPNVPTIRAAKVQ	EF015886
EV99	GPYTGLPTRKPNVPTIRTAKVQ	EF555644
CVA1	GAYTGLPNAKPKVPTIRAAKVQ	AFQ55937
CVA22	GAYTGLPNVKPKVPTIRAAKVQ	AF499643
.	*:*:*:* *:::*::*:*:**	

*100% conserved positions; :similar

Fig. 1. Sequences of EV VPgs used to design the PCP-consensus VPg with their gene bank accession numbers. Only the unique sequences were used in calculating the consensus.

replication (Ambros and Baltimore, 1978; Lee et al., 1977). A uridylylated form of VPg, VPgpUpU, was shown to be present in the cytoplasm of infected cells (Crawford and Baltimore, 1983). Subsequently, it was shown that VPgpU could be formed in an in vitro reaction containing the polymerase (3D^{pol}) and a template RNA. The uridylylated peptides, VPgpU or VPgpUpU, prime viral RNA synthesis (Paul et al., 1998). VPg sequences are present in the genomes of all picornaviruses. Larger VPg proteins were also identified in caliciviruses and other families that were even more distinct from the picornaviruses (Goodfellow, 2011) but which may have arisen from combinations of picornavirus gene sequences during evolution of the eukaryotic cell (Koonin et al., 2008).

A wealth of data indicates that mutations throughout the 22 amino acid sequence of PV1-VPg reduce uridylylation in vitro and lower or eliminate the formation of infectious virus (Kuhn et al., 1988a, 1988b; Paul et al., 2003). However, there are many gene sequences known for EV VPgs, which differ at positions (when aligned with PV-VPg) that are known to affect uridylylation (Fig. 1). Deep sequencing of viral isolates may reveal even more diversity (Acevedo et al., 2014), introduced through the high mutation rate of viral 3D^{pol} (Gnadig et al., 2012). Indeed, VPg seems to be evolving at a very rapid rate, as the sequences of the

four EV 3D^{pol} included here are much more conserved, ranging from 67–74% identity.

However, function eventually constrains sequence variability. To determine the minimum requirements for uridylylation, we analyzed the sequences, the underlying conservation of physico-chemical properties, and the structures of VPg and their binding sites on the polymerases in co-crystal structures. VPg, before uridylylation, in solution has a flexible, or even disordered structure (Schein et al., 2006a), which might also be stabilized by binding to cellular components or the polymerase. In contrast, chemically synthesized uridylylated PV-VPgpU has a very stable structure in solution (Schein et al., 2010). The NMR structure indicated that the positively charged residues directly coordinate with the UMP moiety of the modified tyrosine. Such a stable structure is probably needed for VPgpU to effectively prime RNA synthesis.

To determine the specificity endowed within the diversity of sequences of VPg, we chose four diverse EV polymerases and determined whether they could recognize VPgs that differed greatly in sequence from their own encoded peptide. We purified the 3D^{pol} of three important human pathogens, from EV-A71 (species A), CVB3 (species B), and CVA24 (species C, and closely related in sequence to PV-3D^{pol}) (Smura et al., 2014). Our results indicate that the diversity in the sequences of the VPg of species A–C correlates with their different binding sites for uridylylation on the 3D^{pol}. The underlying physical chemical properties of the VPgs were captured in a single consensus sequence. All four of the polymerases tested could uridylylate this artificial sequence, while still showing preference for their own VPg. The ability of all to uridylylate a consensus peptide, coupled with evidence that VPg-based replication can be done in trans (Chen et al., 2013), suggests that there is indeed a common mechanism for VPg uridylylation. However, the specificity we show here, coupled with the different binding sites seen in co-crystal structures, supports a "2 molecule mechanism" (Sun et al., 2012), where the VPg can be located at different positions on one polymerase molecule, and uridylylated by a second polymerase molecule.

Results

Deriving a PCP-consensus VPg for EV species A–C

The sequences of 31 diverse EV were used to derive a PCP-consensus for VPg (Fig. 1). Only 9 residues (without inserting gaps) of the 22 are conserved across EV species A, B, and C. Seven of these residues are also conserved in analogous positions in diverse Rhinoviruses (RV, enterovirus species D; Table 1). The conservation of G1 and Q22 reflects the sequence needed for protease cleavage of the P3 domain of the polyprotein (Pathak et al., 2007). Despite the relatively low absolute identity, the physical chemical properties at each position are more conserved. For example, there is always a positively charged residue at positions 8–10 in the sequences, and arginine is always present at position 17. The absolute sequence number of the positively charged residues is not conserved (e.g., K9 is a Q, N, R or T in the different sequences). However, all 5 VPg sequences synthesized for this study have the same predicted IEP (10.9) and charge (+4) at pH 7.

The unique VPg sequences (from species A, B, and C) chosen for this study are compared in Table 1 with those of other picornavirus sequences and the uridylylation site of larger VPgs from other virus families. The IEP and net charges for the sequences of RV VPgs are somewhat lower. The sequences of the three genome encoded VPgs of the distantly related Foot and mouth disease virus (FMDV; genus Aphthovirus) are, like FMDV polymerase (see the alignments in Fig. S3), significantly different from those of the

Table 1
Comparison of the isoelectric points (IEP) and net charges at pH 7 of VPgs.

Virus	VPg sequence	IEP	Charge
EV-A71	GAY**S**G**A**P**K**Q**VLKK**P**A**L**RTA**T**VQ	10.9	4
CVB3	GAYTG**V**PN**Q**KP**RV**P**T**LR**Q**AKVQ	11.5	4
PV1	**GAYTGLPNKKPNVPTIRTAKVQ**	10.9	4
CVA24	GAYTGLPNKKP**S**VPT**V**RTAKVQ	10.9	4
PCPCon	GAYTGLPN**Q**KP**K**VPTI**R**TAKVQ	10.9	4
RV2	**GPYSGE**PKPKTKV**PE**RR**IVAQ**	10.4	3
RV4	**GPYSGN**PHNKLKA**P**TL**RP**VVV**Q**	10.7	3
RV16	**GPYSGE**PKPKTKV**PE**RR**VVAQ**	10.4	3
RV89	**GPYSGE**PKPKSRA**PE**RR**VVTQ**	10.7	3
FMDV-VPg1	**GPYA**GPLERQRPLKVRAKLPRQE	11.3	4
FMDV-VPg2	**GPYA**GPMERQKPLKVKARAPVVKE	10.6	4
FMDV-VPg3	**GPYA**GPVKKPVALKVKAKNLIVTE	10.5	4
FCV	GTYRGRGVALTDDE**Y**DEWREHNASRK	5.5	−0.9
MNV	GVFRTRG–L**TDEEY**DEFKKRRESRG	9.6	1

The top five VPgs were used in this study. PV1 VPg sequence is bold; residues that differ from it in the other EV sequences chosen for study are bold and italicized. Residues conserved in EV species A–C are underlined. These are followed by VPg sequences from RV and the 3 genome encoded VPgs of the distantly related picornavirus FMDV. The conserved residues in RV that they share with other enteroviruses are bold. The bold residues in the FMDV sequences are those identical to PV1 VPg.

In contrast, as the last two sequences illustrate, the conserved areas (residues 10–30) around the uridylylated Tyr (bold) from the VPg proteins of feline calicivirus (FCV) and murine norovirus (MNV) VPgs (Leen et al., 2013) have completely different IEP and charge, suggesting two different mechanisms for uridylylation. Mutation of the underlined residues in MNV-VPg greatly reduce or prevent VPg uridylylation, VPg-RNA synthesis by the MNV polymerase and virus recovery (Leen et al., 2013).

Arrows indicate the uridylylated Tyrosine. The charges and IEP were calculated with the Peptide property calculator from Innovagen (http://pepcalc.com/ppc.php).

Enteroviruses used in this study. For example, the FMDV VPgs contain at least one negatively charged amino acid. However, their overall IEP and net charge are similar to those of the EVs.

Fig. 2 shows the absolutely conserved residues of the EV-VPgs (maroon) mapped on the NMR structure of VPg (PDB accession code 2BBL (Schein et al. 2006a)), with the uridylylated Tyr3 residues in turquoise. Residues K9/10 are circled, as mutation of both of these residues is lethal for PV replication in culture.

Comparision of uridylyation activities of EV species A–C

Three 3D^{pol} were purified similarly and their ability to uridylylate the VPgs was compared to that of PV-3D^{pol} (purified in another lab) in the most permissive assay for uridylylation, using a polyA template RNA and Mn^{2+} (Fig. 3). Quantitative comparison of the PAGE assays of representative experiments for uridylylation of the 4 natural VPgs (CVA24, CVB3, EV A71, and PV1), and the PCP-consensus VPg, by three polymerases from the three species is shown in Table 2. Within the accuracy of this assay, we can say that each of the polymerases did show preference for its own VPg, with CVA24 consistently being more accepting of sequences that differed from its own. All of the VPgs, including the consensus, were uridylylated to at least 25% of the efficiency of the cognate encoded VPg.

As a control, we also tested another RNA dependent, RNA polymerase, from the Flavivirus Dengue (DENV), in the uridylylation assay with and without consensus VPg. As Fig. S2 shows, DENV polymerase produced large amounts of RNase A-sensitive,

poly U RNA in the uridylylation assay. As expected, it did not produce VPgpU, which was produced by all three enteroviral 3D^{pol} in the same assay mix.

Discussion

We show here that EV 3D^{pol}, chosen from the most diverse members of EV species A–C, are able to uridylylate all four wild type VPgs as well as a PCP-consensus VPg. The efficiency was 25–100% of that seen for their cognate VPgs. Surprisingly, the two most divergent 3D^{pol}, from EV A71 (EV-A representative) and CVB3 (EV-B), still uridylylated the PCP-consensus VPg as well as or better than the wild type VPgs of CVA24 or PV1 (both EV-C). This indicates there is a common framework for uridylylation by even the most divergent EV-3D^{pol}.

These results mirror to some extent the specificity of RV-VPgs. The rhinovirus VPgs differ from those of EV species A–C in length and the presence of negatively charged amino acids (Table 1). Mutations to insert negative charge into PV1 VPg, such as replacing Leu6 with glutamic acid, greatly reduce replication (Cheney et al., 2003). Previous studies have shown that RV2 3D^{pol} can uridylylate the VPgs of diverse RV (Gerber et al., 2001) and PV VPg, but PV 3D^{pol} cannot uridylylate the VPgs of RV2 or RV89 (Paul et al., 2003). The 3D^{pol} of RV16 (Cheney et al., 2003) also uridylylates PV VPg and the reaction is inhibited by the same mutations that inhibit uridylylation by PV 3D^{pol} (Gerber et al., 2001). This again implies a basic common underlying mechanism, with specificity encoded by both the enzyme and the peptide.

Diverse VPg binding sites on the 3D^{pol} of EV A71 (Chen et al., 2013) and CVB3 (Gruez et al., 2008b) suggest a second polymerase molecule may catalyze uridylylation. These sites are both on the "reverse surface" of the polymerase (Figs. S3 and S4). The site identified for CVB3 is near that identified for PV 3D^{pol} by mutagenesis (Lyle et al., 2002) and docking studies (Schein et al., 2006a, 2006b). Since the site for EV A71 is so different, yet both polymerases are able to uridylylate the same VPgs, this suggests that uridylylation is done by a second polymerase molecule, with the VPg bound to the surface of the first. Assuming the VPgs of species B and C continue to bind to approximately the same region on EV A71, alteration of R379 to L, F377 to G and V391 to T on the protein surface could greatly destabilize the binding site, thus lowering the reaction rate. The need for two polymerase molecules to catalyze the reaction has been suggested by several other authors based on different types of data (Gruez et al., 2008a; Sun et al., 2012; Tellez et al., 2006).

The similarity in overall charge of the 3 encoded FMDV VPgs (Table 1) does suggest that this Apthovirus should have the same basic mechanism as the EV for uridylylation. However, the sequence similarity between the two sets of VPgs is very low (3/22 identical, 3/9 identical for the absolutely conserved amino acids). A Blast search of the Refseq database starting from PV1 VPg brings only VPgs for EV species A–D and J within the first 10 sequences, but no FMDV VPg in the top 100 sequences. The same search, beginning with FMDV VPg2 finds FMDV but no EV VPg.

Further, the polymerases diverge in both sequence and structure. The amino acids of the surface sites for the EV VPgs are not present in FMDV 3D^{pol} (Fig. S3). In co-crystal structures of the 3D^{pol} of FMDV with both its free and uridylylated VPg1 (Ferrer-Orta et al., 2006), both VPg and VPgpU were seen fully extended near the active site of the polymerase. Thus the Apthoviruses may indeed have a different mechanism for uridylylation.

Alternatively, much of the data could be explained if the surface site for VPg is simply to aid in cleavage of VPg from the 3BC protein. Higher resolution crystal structures of the EV-polymerases with their uridylylated VPgs might help to resolve these
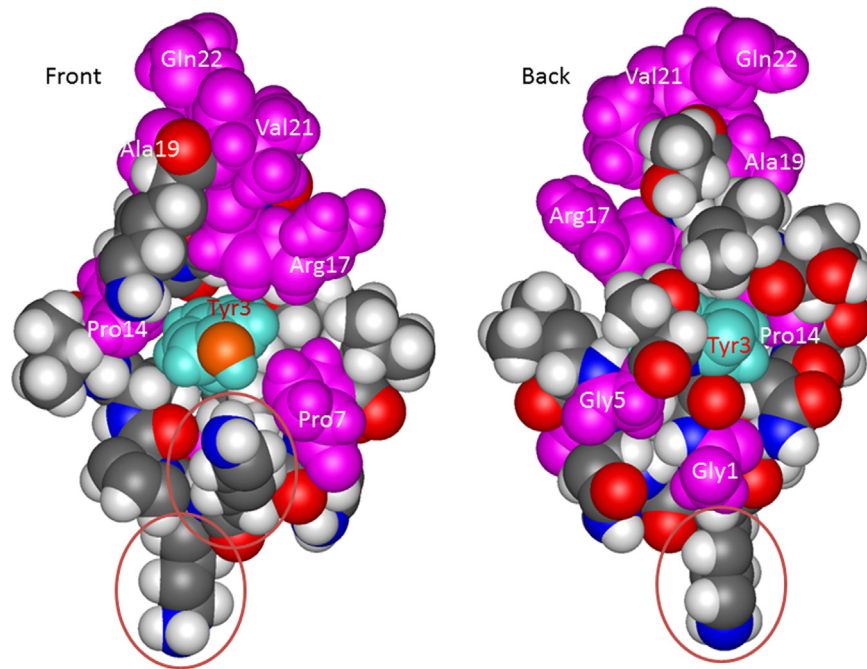
Fig. 2. NMR structure of VPg (2BBL.pdb; structure 1) (Schein et al., 2006a) showing residues conserved in all EV species A–C sequences (maroon) and the uridylylated Tyr3 (in cyan, its phenolic O is in orange red). The other residues are "CPK" colored according to atom type (H=gray, O=red, black=C, Blue=N). Residue positions where positive charge is conserved are circled. Here, Front indicates the (positively charged) face of VPg on which the Tyr3-OH is located, and Back indicates the side of VPg that docks to the polymerase at the indicated binding site for VPg (Schein et al., 2006b).
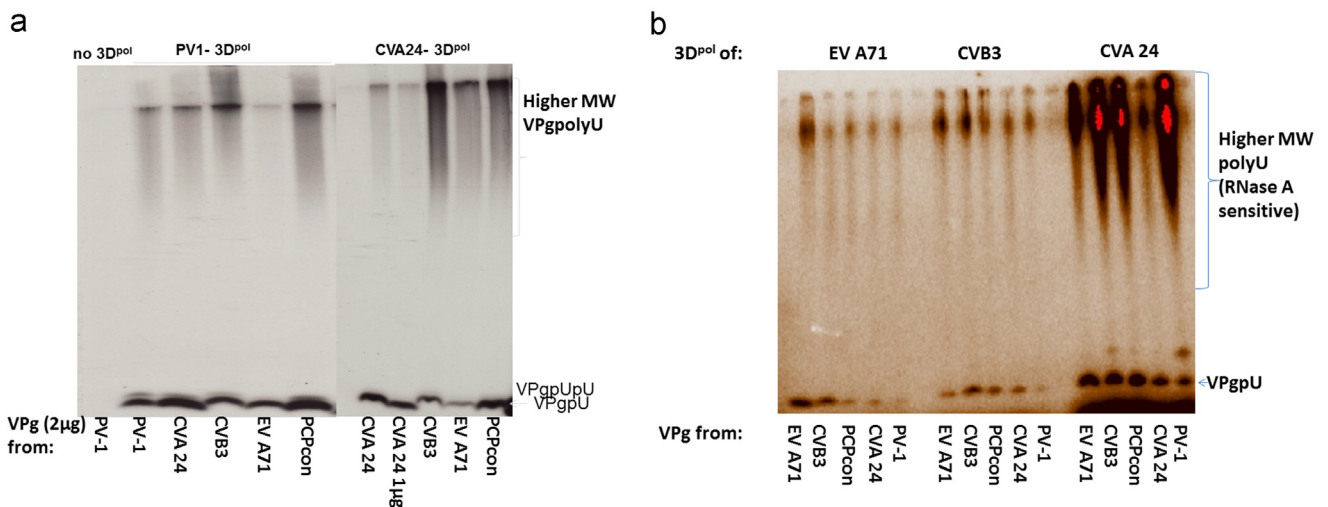
Fig. 3. Uridylation of 5 diverse VPgs by Enteroviral polymerases from species A–C. Sequences of VPgs are shown in Table 1. (a) PV and CVA24 3D^{pol} efficiently uridylylate all five VPgs. The assay was incubated for 1 h at 34 °C, and reactions were run on two − 13.5% PAG (aligned next to one another). Both polymerases from species C (Brown et al., 2003) uridylylate a PCP-consensus VPg (PCPcon) as efficiently as their respective wild-type VPgs and those from EV-B Species B (represented by CVB3 VPg) and species A (EV-A71). (b) Comparison of uridylylation of 5 different VPgs by 3D^{pol} from EV-A71, CVB3, and CVA24. The reactions were incubated for 2 h at 30 °C and run on a 26 slot Criterion Tris–Tricine 10–20% gel (Bio-Rad). The three polymerases were purified within a few weeks of each other (Fig. S1). The reactions were run simultaneously with the same amounts of each VPg in the assay. The quantification is shown in Table 2 products.

possibilities.Essential, negatively charged amino acids in larger VPgs of caliciviruses suggest a different uridylylation mechanism.

It is clear simply from sequence conservation (Table 1), as well as mutation studies, that a net positive charge on the peptide is essential for uridylylation of EV VPgs, and probably for those of FMDV. The positively charged residues could bind the incoming UTP residue during uridylylation, as well as stabilize the position of the bound Tyr-UMP conjugate during priming (Schein et al., 2010).

Although the small picornaviral VPgs are positively charged, the reactive tyrosine in the NMR structures of feline calicivirus (FCV) and murine norovirus (MNV) projects from a protein helix, and is surrounded by negatively charged residues in the linear sequence (last lines of Table 1). As Table 1 shows, the charges of the sequences surrounding the reactive Tyrosine of the FCV and MNV VPgs are "polar opposites". While the positive charges of PV-VPg are essential, mutation of negatively charged residues near the uridylylated Tyr in MNV VPgs prevents formation of the VPg-RNA covalent complex and virus replication (Leen et al., 2013). These residues could stabilize the structure through salt bridges (formed perhaps to residues not included in the NMR structure). Alternatively, they could bind metal ions as part of the catalytic mechanism. Negatively charged amino acids, particularly aspartates, capable of tightly binding metal ions, play an important role in

Table 2
Volumes of the VPg-pU bands and the relative incorporation of P32-UMP into VPgpU/VPgpUpU bands.

3Dpol/VPg	VPg-pU	
CVA24/CVA24VPg	**54,134**	**1.00**
CVA24/CVB3VPg	82,568	1.53
CVA24/EV A71VPg	10,6020	1.96
CVA24/PCPconVPg	99,805	1.84
CVA24/PV1-VPg	33,164	0.61
CVB3/CVA24VPg	17,090	0.54
CVB3/CVB3VPg	**31,852**	**1.00**
CVB3/EV A71VPg	11,040	0.35
CVB3/PCPconVPg	15,722	0.49
CVB3/PV1-VPg	13,223	0.42
EV A71/CVA24VPg	12,208	0.25
EV A71/CVB3VPg	23,309	0.48
EV A71/EV A71VPg	**48,621**	**1.00**
EV A71/PCPconVPg	16,776	0.35
EV A71/PV1-VPg	13,903	0.29

The volumes for the VPgpU bands (see Fig. 3) are given in total units (to allow comparison from one polymerase to the other) and then relative to the wild type VPg for each 3D^{pol} (shown bold). Results with the consensus VPg are underlined for each 3D^{pol}.

nuclease and phosphatase common mechanisms (Braun and Schein, 2014; Oezguen et al., 2007).

The differences in the environment of the uridylylated tyrosine in different VPgs suggests that the "big bang of picornavirus evolution" (Koonin et al., 2008) that gave rise to so many diverse viruses, also gave different solutions to the problem of generating a stable surface to prime RNA synthesis.

Methods

VPg synthesis and quantification

VPgs were produced synthetically, using normal FMOC-based amino acid derivatives. Synthetic VPgpU, used for calibrating the position of VPgpU on gels in early stages of this work, was generated as described previously (Schein et al., 2010; van der Heden van Noort et al., 2013). VPgs were dissolved in water and their concentration determined using the extinction coefficients for tyrosine (the only UV-absorbing amino acid in the peptide) in the range of 220–280 nm.

Determining a PCP-consensus VPg

The PCP-consensus method determines the sequence that is most similar in its physical chemical properties to all others in a set. It is designed to be useful for sets with many sequences (such as viral isolates) that have a high superficial redundancy (i.e., nearly identical sequences that differ at only a few positions). The rationale and details of the method are described in detail elsewhere (Bowen et al., 2012; Danecek et al., 2010; Danecek and Schein, 2010; Schein et al., 2012). Here, the PCP-con program was used to determine a consensus of 31 of the most diverse EV VPg sequences (Fig. 1). The resulting PCP-consensus sequence is compared to the four wild type VPgs that were used in this study in Table 1.

Polymerase purification

Genes for the CVA24 and EV A71 polymerases were obtained from EV collections at the CDC. The CVB3 polymerase gene was obtained from the cloned cDNA of the strain CVB3/28 (Tu et al.,

1995). This strain induces myocarditis and pancreatitis in susceptible mice and accelerates the development of T1 diabetes in older non-obese diabetic mice (Tracy et al., 2002). The three 3D^{pol} genes were subcloned into pET30 in the Recombinant DNA Laboratory at UTMB, so that the resulting protein would have a C-terminal hexahistidine tag. PV 3D^{pol} was expressed in *Escherichia coli* from plasmid pT5-3D (a gift of Dr. Karla Kirkegaard).

Plasmids containing the respective 3D^{pol} gene were transformed into the Rosetta DE3 strain of *E. coli* that has been optimized for the codon usage of higher organisms. Protein expression was induced with 1 mM isopropyl β-D-thiogalactopyranoside (IPTG) for 16 hours at 18 °C (with shaking). The 3D^{pol} was in the soluble fraction of the lysate and was purified using Talon metal affinity resin (Clontech) with a 5–100 mM imidazole gradient. Protein-containing fractions were concentrated to ~2 mL, and further purified on a Superdex 75 (GE Healthcare) gel filtration column. Protein-containing fractions were pooled and concentrated to 2–7 mg/mL (Fig. S1). Dengue virus polymerase was expressed and purified as described previously (Bussetta and Choi, 2012).

Assay for uridylylation

The reaction mixtures (10 μl) contained 50 mM HEPES, pH 7.5, 8% glycerol, 0.5 μg of the template RNA: polyA (Sigma); 0.5 mM manganese(II) acetate, 1–2 μg purified 3D^{pol}, 1 μg synthetic VPg, and 10 μM UTP (+α-UT^{32}P (Amersham)) (Paul et al., 1998). Except where noted otherwise (Fig. 3a), multiplex assays of the polymerases with the five VPgs were done in siliconized PCR plates and incubated for 2 h at 30 °C. They were stopped by addition of SDS containing gel loading buffer and heated at 60 °C for 3–4 min before applying to TGX-any KD minigels (15 slot) or Criterion (26 slot), Tris–Tricine/SDS-PAGE (10–20%, Biorad Criterion Peptide). The uridylylated VPg^{32}pU products were quantified with a Phosphorimager (PMI; Biorad).

Appendix A. Supporting information

Supplementary data associated with this article can be found in the online version at http://dx.doi.org/10.1016/j.virol.2015.05.016.

References

Abzug, M.J., 2014. The enteroviruses: problems in need of treatments. J. Infect. 68 (Suppl. 1), S108–S114.

Acevedo, A., Brodsky, L., Andino, R., 2014. Mutational and fitness landscapes of an RNA virus revealed through population sequencing. Nature 505, 686–690.

Ambros, V., Baltimore, D., 1978. Protein is linked to the 5′ end of poliovirus RNA by a phosphodiester linkage to tyrosine. J. Biol. Chem. 253, 5263–5266.

Blomqvist, S., Paananen, A., Savolainen-Kopra, C., Hovi, T., Roivainen, M., 2008. Eight years of experience with molecular identification of human enteroviruses. J. Clin. Microbiol. 46, 2410–2413.

Bowen, D.M., Lewis, J.A., Lu, W., Schein, C.H., 2012. Simplifying complex sequence information: a PCP-consensus protein binds antibodies against all four Dengue serotypes. Vaccine 30, 6081–6087.

Braun, W., Schein, Catherine H., 2014. Membrane interaction and functional plasticity of inositol polyphosphate 5-phosphatases. Structure 22, 664–666.

Brown, B., Oberste, M.S., Maher, K., Pallansch, M.A., 2003. Complete genomic sequencing shows that polioviruses and members of human enterovirus species C are closely related in the noncapsid coding region. J. Virol. 77, 8973–8984.

Bussetta, C., Choi, K.H., 2012. Dengue virus nonstructural protein 5 adopts multiple conformations in solution. Biochemistry 51, 5921–5931.

Campagnola, G., Gong, P., Peersen, O.B., 2011. High throughput screening identification of poliovirus RNA-dependent RNA polymerase inhibitors. Antivir. Res. 91, 241–251.

Chan, Y.F., Sam, I.C., Wee, K.L., Abubakar, S., 2011. Enterovirus 71 in Malaysia: a decade later. Neurol. Asia 16, 1–15.

Chapman, N.M., Kim, K.S., 2008. Persistent coxsackievirus infection: enterovirus persistence in chronic myocarditis and dilated cardiomyopathy. Curr. Top. Microbiol. Immunol. 323, 275–292.

Chen, C., Wang, Y., Shan, C., Sun, Y., Xu, P., Zhou, H., Yang, C., Shi, P.-Y., Rao, Z., Zhang, B., Lou, Z., 2013. Crystal structure of enterovirus 71 RNA-dependent RNA polymerase complexed with its protein primer VPg: implication for a trans mechanism of VPg uridylylation. J. Virol. 87, 5755–5768.

Cheney, I.W., Naim, S., Shim, J.H., Reinhardt, M., Pai, B., Wu, J.Z., Hong, Z., Zhong, W., 2003. Viability of poliovirus/rhinovirus VPg chimeric viruses and identification of an amino acid residue in the VPg gene critical for viral RNA replication. J. Virol. 77, 7434–7443.

Cooper Jr., L.T., 2009. Myocarditis. N. Engl. J. Med. 360, 1526–1538.

Crawford, N.M., Baltimore, D., 1983. Genome-linked protein VPg of poliovirus is present as free VPg and CPgpUpU in poliovirus-infected cells. Proc. Natl. Acad. Sci. USA 80, 7452–7455.

Danecek, P., Lu, W., Schein, C.H., 2010. PCP consensus sequences of flaviviruses: correlating variance with vector competence and disease phenotype. J. Mol. Biol. 396, 550–563.

Danecek, P., Schein, C.H., 2010. Flavitrack analysis of the structure and function of West Nile non-structural proteins. Int. J. Bioinform. Res. Appl. 6, 134–146.

Eyckmans, T., Wollants, E., Janssens, A., Schoemans, H., Lagrou, K., Wauters, J., Maertens, J., 2014. Coxsackievirus A16 encephalitis during obinutuzumab therapy, Belgium. Emerg. Infecti. Dis. 20, 913–915.

Ferrer-Orta, C., Arias, A., Agudo, R., Perez-Luque, R., Escarmis, C., Domingo, E., Verdaguer, N., 2006. The structure of a protein primer-polymerase complex in the initiation of genome replication. EMBO J. 25, 880–888.

Gerber, K., Wimmer, E., Paul, A.V., 2001. Biochemical and genetic studies of the initiation of human rhinovirus 2 RNA replication: purification and enzymatic analysis of the RNA-dependent RNA polymerase 3Dpol. J. Virol. 75, 10969–10978.

Gnadig, N.F., Beaucourt, S., Campagnola, G., Borderia, A.V., Sanz-Ramos, M., Gong, P., Blanc, H., Peersen, O.B., Vignuzzi, M., 2012. Coxsackievirus B3 mutator strains are attenuated in vivo. Proc. Natl. Acad. Sci. USA 109, E2294–2303.

Goodfellow, I., 2011. The genome-linked protein VPg of vertebrate viruses – a multifaceted protein. Curr. Opin. Virol. 1, 355–362.

Gruez, A., Selisko, B., Roberts, M., Bricogne, G., Bussetta, C., Jabafi, I., Coutard, B., De Palma, A.M., Neyts, J., Canard, B., 2008a. The crystal structure of coxsackievirus B3 RNA-dependent RNA polymerase in complex with its protein primer VPg confirms the existence of a second VPg binding site on Picornaviridae polymerases. J. Virol. 82, 9577–9590.

Gruez, A., Selisko, B., Roberts, M., Bricogne, G., Bussetta, C., Jabafi, I., Coutard, B., De Palma, A.M., Neyts, J., Canard, B., 2008b. The crystal structure of coxsackievirus B3 RNA-dependent RNA polymerase in complex with its protein primer VPg confirms the existence of a second VPg binding site on Picornaviridae polymerases. J. Virol. 82, 9577–9590.

Jacobson, L.M., Redd, J.T., Schneider, E., Lu, X., Chern, S.W., Oberste, M.S., Erdman, D. D., Fischer, G.E., Armstrong, G.L., Kodani, M., Montoya, J., Magri, J.M., Cheek, J.E., 2012. Outbreak of lower respiratory tract illness associated with human enterovirus 68 among American Indian children. Pediatr. Infect. Dis. J. 31, 309–312.

Koonin, E.V., Wolf, Y.I., Nagasaki, K., Dolja, V.V., 2008. The Big Bang of picorna-like virus evolution antedates the radiation of eukaryotic supergroups. Nat. Rev. Microbiol. 6, 925–939.

Kreuter, J.D., Barnes, A., McCarthy, J.E., Schwartzman, J.D., Oberste, M.S., Rhodes, C. H., Modlin, J.F., Wright, P.F., 2011. A fatal central nervous system enterovirus 68 infection. Arch. Pathol. Lab. Med. 135, 793–796.

Kuhn, R.J., Tada, H., Ypma-Wong, M.F., Dunn, J.J., Semler, B.L., Wimmer, E., 1988a. Construction of a "mutagenesis cartridge" for poliovirus genome-linked viral protein: isolation and characterization of viable and nonviable mutants. Proc. Natl. Acad. Sci. USA 85, 519–523.

Kuhn, R.J., Tada, H., Ypma-Wong, M.F., Semler, B.L., Wimmer, E., 1988b. Mutational analysis of the genome-linked protein VPg of poliovirus. J. Virol. 62, 4207–4215.

Lee, Y.F., Nomoto, A., Detjen, B.M., Wimmer, E., 1977. A protein covalently linked to poliovirus genome RNA. Proc. Natl. Acad. Sci. USA 74, 59–63.

Leen, E.N., Kwok, K.Y.R., Birtley, J.R., Simpson, P.J., Subba-Reddy, C.V., Chaudhry, Y., Sosnovtsev, S.V., Green, K.Y., Prater, S.N., Tong, M., Young, J.C., Chung, L.M.W., Marchant, J., Roberts, L.O., Kao, C.C., Matthews, S., Goodfellow, I.G., Curry, S., 2013. Structures of the compact helical core domains of feline calicivirus and murine norovirus VPg proteins. J. Virol. 87, 5318–5330.

Lyle, J.M., Clewell, A., Richmond, K., Richards, O.C., Hope, D.A., Schultz, S.C., Kirkegaard, K., 2002. Similar structural basis for membrane localization and protein priming by an RNA-dependent RNA polymerase. J. Biol. Chem. 277, 16324–16331.

Moturi, E.K., Porter, K.A., Wassilak, S.G., Tangermann, R.H., Diop, O.M., Burns, C.C., Jafari, H., 2014. Progress toward polio eradication–worldwide, 2013–2014. MMWR Morb Mortal Wkly Rep 63. pp. 468–472.

Oezguen, N., Schein, C.H., Peddi, S.R., Power, T.D., Izumi, T., Braun, W., 2007. A "moving metal mechanism" for substrate cleavage by the DNA repair endonuclease APE-1. Proteins 68, 313–323.

Pallansch, M.A., Oberste, M.S., Whitton, J.L., 2013. Enteroviruses: polioviruses, coxsackieviruses, echoviruses, and newer enteroviruses. In: Knipe, DM, Cohen, H.P., Griffin, JI, Lamb, DE, Martin, RA, Roizman B., MA (Eds.), Fields Virology, 6th ed. Lippincott Williams & Wilkins, Philadelphia.

Pathak, H.B., Arnold, J.J., Wiegand, P.N., Hargittai, M.R.S., Cameron, C.E., 2007. Picornavirus genome replication – assembly and organization of the VPg uridylylation ribonucleoprotein (initiaion) complex. J. Biol. Chem. 282, 16202–16213.

Paul, A.V., Peters, J., Mugavero, J., Yin, J., van Boom, J.H., Wimmer, E., 2003. Biochemical and genetic studies of the VPg uridylylation reaction catalyzed by the RNA polymerase of poliovirus. J. Virol. 77, 891–904.

Paul, A.V., van Boom, J.H., Filippov, D., Wimmer, E., 1998. Protein-primed RNA synthesis by purified poliovirus RNA polymerase. Nature 393, 280–284.

Salvatoni, A., Baj, A., Bianchi, G., Federico, G., Colombo, M., Toniolo, A., 2013. Intrafamilial spread of enterovirus infections at the clinical onset of type 1 diabetes. Pediatr. Diabetes 14, 407–416.

Schein, C.H., Bowen, D.M., Lewis, J.A., Choi, K., Paul, A., van der Heden van Noort, G. J., Lu, W., Filippov, D.V., 2012. Physicochemical property consensus sequences for functional analysis, design of multivalent antigens and targeted antivirals. BMC Bioinform. 13 (Suppl. 13), S9.

Schein, C.H., Oezguen, N., van der Heden van Noort, G.J., Filippov, D.V., Paul, A., Kumar, E., Braun, W., 2010. NMR solution structure of poliovirus uridylylated peptide linked to the genome (VPgpU). Peptides 31, 1441–1448.

Schein, C.H., Oezguen, N., Volk, D.E., Garimella, R., Paul, A., Braun, W., 2006a. NMR structure of the viral peptide linked to the genome (VPg) of poliovirus. Peptides 27, 1676–1684.

Schein, C.H., Volk, D.E., Oezguen, N., Paul, A., 2006b. Novel, structure-based mechanism for uridylylation of the genome-linked peptide (VPg) of picornaviruses. Proteins 63, 719–726.

Smura, T., Blomqvist, S., Vuorinen, T., Ivanova, O., Samoilovich, E., Al-Hello, H., Savolainen-Kopra, C., Hovi, T., Roivainen, M., 2014. Recombination in the evolution of enterovirus C species sub-group that contains types CVA-21, CVA-24, EV-C95, EV-C96 and EV-C99. PLoS One 9, e94579.

Stephenson, J., 2014. CDC tracking enterovirus D-68 outbreak causing severe respiratory illness in children in the Midwest. JAMA 312, 1290.

Sun, Y., Wang, Y., Shan, C., Chen, C., Xu, P., Song, M., Zhou, H., Yang, C., Xu, W., Shi, P.-Y., Zhang, B., Lou, Z., 2012. Enterovirus 71 VPg uridylation uses a two-molecular mechanism of 3D polymerase. J. Virol. 86, 13662–13671.

Tao, Z., Wang, H., Li, Y., Liu, G., Xu, A., Lin, X., Song, L., Ji, F., Wang, S., Cui, N., Song, Y., 2014. Molecular epidemiology of human enterovirus associated with aseptic meningitis in Shandong Province, China, 2006–2012. PLoS One 9, e89766.

Tellez, A.B., Crowder, S., Spagnolo, J.F., Thompson, A.A., Peersen, O.B., Brutlag, D.L., Kirkegaard, K., 2006. Nucleotide channel of RNA-dependent RNA polymerase used for intermolecular uridylylation of protein primer. J. Mol. Biol. 357, 665–675.

Tokarz, R., Firth, C., Madhi, S.A., Howie, S.R., Wu, W., Sall, A.A., Haq, S., Briese, T., Lipkin, W.I., 2012. Worldwide emergence of multiple clades of enterovirus 68. J. Gen. Virol. 93, 1952–1958.

Tracy, S., Drescher, K.M., Chapman, N.M., Kim, K.S., Carson, S.D., Pirruccello, S., Lane, P.H., Romero, J.R., Leser, J.S., 2002. Toward testing the hypothesis that group B coxsackieviruses (CVB) trigger insulin-dependent diabetes: inoculating non-obese diabetic mice with CVB markedly lowers diabetes incidence. J. Virol. 76, 12097–12111.

Tu, Z., Chapman, N.M., Hufnagel, G., Tracy, S., Romero, J.R., Barry, W.H., Zhao, L., Currey, K., Shapiro, B., 1995. The cardiovirulent phenotype of coxsackievirus B3 is determined at a single site in the genomic 5′ nontranslated region. J. Virol. 69, 4607–4618.

van der Heden van Noort, G.J., Schein, C.H., Overkleeft, H.S., van der Marel, G.A., Filippov, D.V., 2013. A general synthetic method toward uridylylated picornavirus VPg proteins. J. Pept. Sci. 19, 333–336.

Wang, Y., Zhu, Q., Zeng, M., Altmeyer, R., Zou, G., 2014. Complete genome sequence of a human enterovirus 71 strain isolated from a fatal case in Shanghai, China, in 2012. Genome Announc. 2 (3), pii: e00457-14 (22 May 2014).

Yeung, W.C., Rawlinson, W.D., Craig, M.E., 2011. Enterovirus infection and type 1 diabetes mellitus: systematic review and meta-analysis of observational molecular studies. BMJ 342, d35.

Yu, P., Gao, Z., Zong, Y., Bao, L., Xu, L., Deng, W., Li, F., Lv, Q., Xu, Y., Yao, Y., Qin, C., 2014. Histopathological features and distribution of EV71 antigens and SCARB2 in human fatal cases and a mouse model of enterovirus 71 infection. Virus Res. 189, 121–132.

Zheng, X.Q., Chen, X.Q., Gao, Y., Fu, M., Chen, Y.P., Xu, D.P., Lin, A., Yan, W.H., 2014. Elevation of human leukocyte antigen-G expression is associated with the severe encephalitis associated with neurogenic pulmonary edema caused by Enterovirus 71. Clin. Exp. Med. 14, 161–167.